Geodesics of Linear Dilaton Black Holes

Alan Hameed Hussein Hamo

Submitted to the
Institute of Graduate Studies and Research
in partial fulfillment of the requirements for the Degree of

Master of Science
in
Physics

Eastern Mediterranean University
August 2014
Gazimağusa, North Cyprus

Approval of the Institute of Graduate Studies and Research

Prof. Dr. Elvan Yılmaz
Director

I certify that this thesis satisfies the requirements as a thesis for the degree of Master of Science in Physics.

Prof. Dr. Mustafa Halilsoy
Chair, Department of Physics

We certify that we have read this thesis and that in our opinion it is fully adequate in scope and quality as a thesis for the degree of Master of Science in Physics.

Assoc. Prof. Dr. İzzet Sakallı
Supervisor

Examining Committee

1. Prof. Dr. Mustafa Halilsoy _____

2. Assoc. Prof. Dr. Habib Mazharimousavi _____

3. Assoc. Prof. Dr. İzzet Sakallı _____

ABSTRACT

In this thesis, we investigate the geodesics of the 4-dimensional (4D) linear dilaton black hole (LDBH), which is an exact solution to the Einstein-Maxwell-Dilaton (EMD) theory. These spacetimes have non-asymptotically flat (NAF) geometry. The motions of massless (null) and massive particles (timelike) are studied via the standard Lagrangian method. Due to the physical necessities, we do not consider the spacelike geodesics. After obtaining the Euler-Lagrange (EL) equations, we separately analyze both radial and circular motions of those geodesics. In the same line of thought, we perform numerical simulations in order to plot many graphs for displaying the geodesics. Exact analytical solutions are also obtained for the radial and the angular geodesic equations. In particular, it is shown that the radial trajectories are governed by the WeierstrassP-function ($\wp$-function), which is an elliptic-type special function.

Keywords: Linear dilaton black hole, Geodesics, WeierstrassP-function.

ÖZ

Bu tezde, Einstein-Maxwell-Dilaton (EMD) teorisinin tam bir çözümü olan 4-boyutlu (4D) doğrusal dilaton kara deliğinin (LDBH) jeodeziklerini araştırmaktayız. Bu uzay-zamanları asimptotik düz-olmayan (NAF) geometriye sahiptirler. Kütlesiz (boş) ve kütleli parçacıkların (zaman-gibi) jeodezik hareketleri standart Lagrange yöntemi ile incelenmiştir. Fiziksel gereklilikten ötürü, uzay-gibi jeodezikleri dikkate almadık. Euler-Lagrange (EL) denklemlerini elde ettikten sonra, radyal ve dairesel jeodeziklerin her ikisini de ayrı ayrı analiz ettik. Bu düşünce doğrultusunda, jeodeziklerin görüntülenmesi sağlaycak birçok grafik çizebilmek için nümerik simulasyonlar yaptık. Radyal ve açısal jeodezik denklemleri için tam analitik çözümler ayrıca elde edilmiştir. Özellikle, radyal yörüngelerin eliptik-tipi özel bir fonksiyon olan WeierstrassP-fonksiyonu ($\wp$-fonksiyonu) tarafından yönetildiği gösterdik.

Anahtar kelimeler: Lineer dilaton kara deliği, Jeodezik, WeierstrassP-fonksiyonu.

DEDICATION

I dedicate this humble effort:

To the prophet of this nation

and its bright light Mohammad

To the source of kindness

My dear mother and father

To those who reside in my heart

My brothers and sisters

To My supervisor

And finally to all nice people

ACKNOWLEDGMENT

"In the Name of God, Most Gracious and Most Merciful".

First of all I am thankful to God for helping me to fulfill this work.

I would like to express our deep gratitude and sincere appreciation to our project supervisor, Assoc. Prof. Dr. İzzet Sakallı. I am deeply thankful to Prof. Dr Mustafa Halilsoy and Assoc. Prof. Dr. Habib Mazharimousavi for their effort in teaching me numerous basic knowledge concepts in Physics.

I should express many thanks to the faculty members of the Physics Department, especially for Prof. Dr. Özay Gürtuğ.

I also would like to thank our colleagues and friends in the Physics Department. Their invaluable help and personal support are deeply appreciated.

TABLE OF CONTENTS

ABSTRACT iii

ÖZ iv

DEDICATION v

ACKNOWLEDGMENT vi

LIST OF FIGURES ix

1 INTRODUCTION.....1

2 LDBH SPACETIME 3

3 RADIAL GEODESICS OF THE LDBH 6

3.1 Derivation of the Complete Geodesics Equations of the LDBH From EL Equations 6

3.2 Radial Geodesics Without Angular Momentum 8

4 CIRCULAR GEODESICS OF THE LDBH 15

4.1 Geodesics With Angular Momentum 15

4.2 Null Geodesics of the Circular Motion 17

4.3 Timelike Geodesics of the Circular Motion 21

5 ANALYTIC SOLUTION TO THE GEODESIC EQUATIONS OF THE LDBH GEOMETRY 24

5.1 EL Equations With Mino Proper Time 24

5.2 Exact Analytical Solution of the Radial Geodesics 25

5.3 Exact Analytical Solution of the Angular Geodesics 28

6 CONCLUSION.....39

REFERENCES.....30

LIST OF FIGURES

Figure 1: The plot of the effective potential $V_{eff}(\hat{r})$ versus $\hat{r}$. The plot is governed by [Eq. (3.25)]. For a constant $\hat{M}$, the linear behavior of the $V_{eff}(\hat{r})$ is illustrated 12

Figure 2: Plot of how the massive particle falls into $r = 0$ singularity of the LDBH spacetime. The plots are governed by Eqs. (3.20) and (3.27) 13

Figure 3: A plot E^2 versus r_i [Eq. (3.29)] of a massive particle, starting from rest at r_i, which moves along timelike geodesics for different values of r_0. Here b=1 14

Figure 4: The plot of $\tilde{V}_{eff}$ versus $\tilde{r}$ [see Eq. (4.13)]. For various r_0 values, it is seen that there exists unstable orbits for the massless particles (photons). However, the instability tends to disappear for the greater values r_0 while $\tilde{r} \to \infty$ 19

Figure 5: Circular orbits of the photons. The simulations which are made in the famous mathematical program Maple 18 [19] are governed by Eq. (3.11) with $\varepsilon = 0$. During simulations, the initial speed of the photon is assumed to be 1, and the Runge-Kutta method is employed. The far region (a), the middle region (b) and the near horizon region behaviors of the photon are shown. Parameters are chosen to be $M = 1$ $(\because\ r_h = 4)$ and $\ell^2 = 10$. 20

Figure 6: The V_{eff} plot versus $\tilde{r}$ for massive particles with different values of r_0. No stable orbits exist. Here $M = 1$. 21

Figure 7: Circular orbits of the massive particles for various r_0 values. The simulations are performed with the Maple 18 [19] and they are governed by Eq.

(3.11) with $\varepsilon = -1$. During simulations, the initial speed of the massive particle is assumed to be 0, and the Runge-Kutta method is employed. Parameters are chosen to be $M = 1$ $\left(\therefore\ r_h = 4\right)$ and $\ell^2 = 10$. 22

Figure 8: Plots of the circular velocity $v_{\square}$ versus radial distance r for different values of the r_0. The blue dashed line indicates the event horizon. 23

Chapter 1

INTRODUCTION

The motion of test particles (both massive and massless) provides the only experimentally feasible way to study the gravitational fields of objects such as black holes (BHs). Predictions about their observable effects (light deflection, the perihelion shift, gravitational time–delay etc.) can be made, and also compared with the observations. For this reason, geodesics in the BH spacetimes have always been studied, extensively. Today, there are numerous studies about the geodesics of various BHs in the literature (for instance, one may see [1]). Recently, exploring the general solution to the geodesic equation in 4D spacetimes has also been attracted much attention [2-5].

In this thesis, our main motivation is to study the geodesic structure of the LDBH introduced in [6] whose asymptotic behavior is NAF. This BH arises as an exact solution to the EMD theory [6,7]. One of the intriguing features of these BHs is that their Hawking radiation (HR) is governed by isothermal processes, which occur at a constant temperature. Namely, while a LDBH radiates, the energy transferring out of the BH happens at such a slow rate that the thermal equilibrium is always maintained. The thermodynamical studies on the LDBH can be seen in [8-14].We study the motion of both massless (null geodesics) and massive particles (timelike geodesics) on this background. To this end, we follow the standard Lagrangian procedure as employed in [5]. We analyze the effective potential, which describes

the motion of particles along the null and timelike geodesics. We make numerical computations and present many plots to serve fine details about the associated geodesics. Also, we give analytical expressions for the radial and angular geodesic equations. The radial ones are found in terms of the $\wp$-function [15].

The thesis is organized as follows. In chapter 2, we review the LDBH spacetime and present some of its physical properties. In chapter 3, the derivation of geodesic equations via the standard Lagrangian method is represented. Radial geodesics with zero angular momentum are also discussed. Chapter 4 is devoted to the circular motion of the null and timelike geodesics. The plots of those geodesics are exhibited. Exact analytical solutions of the geodesic equations in the LDBH background are studied in chapter 5. We draw our conclusions in chapter 6.

Chapter 2

LDBH SPACETIME

In general, the metric of a static and spherically symmetric BH in 4D is given by:

$$ds^2 = -fdt^2 + f^{-1}dr^2 + R^2 d\Omega^2 \tag{2.1}$$

where

$$d\Omega^2 = d\theta^2 + sin\theta^2 d\phi^2 \tag{2.2}$$

which is the line-element of the unit 2-sphere. When the metric functions of the line-element (2.1) are written in the following form:

$$f = \frac{1}{r_0}(r - b) \tag{2.3}$$

$$R^2 = r_0 r \tag{2.4}$$

the spacetime (2.1) is called as the LDBH. Here, the physical constant parameter r_0 is related with the conserved charge of the LDBH as: $r_0 = \sqrt{2}Q$ in which Q is a non-zero positive definite physical parameter [6]. However, these BHs have no zero charge limit due to the associated field equations coming from the EMD theory. More details about this issue can be found in the paper written by Clément et al. [6].

It is obvious from Eq. (2.3) that a LDBH possesses a NAF geometry and its event horizon is $r_h = b$. For $b \neq 0$, the horizon transparently shields the null singularity at $r = 0$. On the other hand, if one considers the quasi-local mass (M) definition of

Brown and York [16] for the line-element (1) with Eqs. (2.3) and (2.4), we obtain the following relationship

$$b = 4M \tag{2.5}$$

In general, the definition of the Hawking temperature T_H [17] is expressed in terms of the surface gravity κ:

$$\kappa = \sqrt{\left[-\frac{1}{4}\lim_{r\to r_h}\left(g^{tt}g^{ij}g_{tt,i}g_{tt,j}\right)\right]} \tag{2.6}$$

as

$$T_H = \frac{\kappa}{2\pi} \tag{2.7}$$

Using Eq. (2.6), one can compute the surface gravity $\kappa = \frac{1}{2r_0}$. Thus, the T_H value of the LDBH becomes:

$$T_H = \frac{1}{4\pi r_0} \tag{2.8}$$

It is obvious from the above expression that the obtained temperature is constant; thus $\Delta T = 0$. So, the HR of the LDBH is made by the series of the isothermal processes.

One can also compute that the invariants (Ricci scalar ($\Re$), full contradiction of the Ricci tensor ($\Re_{\alpha\beta}\Re^{\alpha\beta}$) and Kretschmann scalar ($\aleph$), see [18] for the details) of the spacetime and obtains

$$\Re = \frac{1}{2r_0}\left(\frac{1}{r} - \frac{b}{r^2}\right) \tag{2.9}$$

$$\mathfrak{R}_{\alpha\beta}\mathfrak{R}^{\alpha\beta} = \frac{1}{4r_0^2}\left(\frac{b^2}{r^4} + \frac{3}{r^2}\right) \tag{2.10}$$

$$\aleph = \mathfrak{R}_{\alpha\beta\mu\nu}\mathfrak{R}^{\alpha\beta\mu\nu} = \frac{1}{4r_0^2}\left(\frac{3b^2}{r^4} + \frac{6b}{r^3} + \frac{11}{r^2}\right) \tag{2.11}$$

which represent that the curvature singularity is located at $r = 0$.

Chapter 3

RADIAL GEODESICS OF THE LDBH

3.1 Derivation of the Complete Geodesics Equations of the LDBH From EL Equations

In order to study the geodesics of the test particles in the LDBH background, in this section we employ the standard Lagrangian method. The corresponding Lagrangian (L) of a massive particle with unit mass in the LDBH geometry is given by

$$2L = -f\dot{t}^2 + \frac{\dot{r}^2}{f} + r_o r\left(\dot{\theta} + sin^2\theta\dot{\phi}^2\right) \tag{3.1}$$

where the dot over a quantity denotes the derivative with respect to the affine parameter σ. The metric condition is in general defined by

$$L = \frac{\varepsilon}{2} \tag{3.2}$$

in which $\varepsilon = 0(-1)$ stands for the null (timelike) geodesics. Since (t,ϕ) are cyclic coordinates, their conjugate momenta $(\Pi_t, \Pi\phi)$ are

$$\frac{d}{d\sigma}\frac{\partial L}{\partial \dot{t}} = \frac{d\Pi_t}{d\sigma} = -\frac{d}{d\sigma}\left(f\dot{t}\right) = 0 \tag{3.3}$$

$$\frac{d}{d\sigma}\frac{\partial L}{\partial \dot{t}} = \frac{d\Pi\phi}{d\sigma} = \frac{d}{d\sigma}\left(r_o r sin^2\theta\dot{\phi}\right) = 0 \tag{3.4}$$

Besides, the metric (2.1) admits a timelike Killing vector field as $\xi = \partial_t$, which is related to the *stationarity* of the metric. Thus, we obtain a conserved quantity as follows.

$$\begin{aligned} & g_{\alpha\beta}\xi^{\alpha}u^{\beta} = -\dot{t}f = -E \\ & \rightarrow \quad \dot{t} = \frac{Er_0}{r-b} \end{aligned} \tag{3.5}$$

where E is a constant of motion and u^{β} is known as the four-velocity vector. This E is related to the energy of the test particles. However, due to the NAF structure of the LDBH spacetime, E is associated with the "total energy" of the particles detected by an external observer located at $r = r_0 + b$, instead of the spatial infinity, which is in general valid for the asymptotically-flat geometries. On the other hand, the spacelike Killing vector $\chi = \partial_{\phi}$ is related to the axial symmetry of the line-element (2.1). Its conserved quantity is found by

$$\begin{aligned} & g_{\alpha\beta}\chi^{\alpha}u^{\beta} = r_o r \sin^2\theta\dot{\phi} = l \\ & \rightarrow \quad \dot{\phi} = \frac{l}{r_o r \sin^2\theta} \end{aligned} \tag{3.6}$$

where l is an integration constant associated with the angular momentum of the particles. For simplicity reasons, we project the problem onto an equilateral plane whose $\theta = \frac{\pi}{2}$. This makes it possible to obtain the following radial EL equation:

$$\left(\frac{dr}{d\sigma}\right)^2 = E^2 - f\left(-\varepsilon + \frac{\ell^2}{r_o r}\right) \tag{3.7}$$

which can be rewritten as

$$\frac{1}{2}\left(\frac{dr}{d\sigma}\right)^2 + V_{eff} = \xi_{eff} \tag{3.8}$$

where the effective potential and the effective energy read

$$V_{eff} = \frac{1}{2} f\left(-\varepsilon + \frac{\ell^2}{r_o r}\right) \tag{3.9}$$

$$\xi_{eff} = \frac{1}{2} E^2 \tag{3.10}$$

Using the chain rule $\frac{d}{d\sigma} = \frac{\ell}{r r_o}\frac{d}{d\phi}$, we obtain

$$\left(\frac{dr}{d\phi}\right)^2 = \frac{2 r_o^{\,2} r^2}{\ell^2}\left(\xi_{eff} - V_{eff}\right). \tag{3.11}$$

Setting $r = \frac{1}{u}$, we can carry out the problem to the standard Kepler problem. Thus, we have

$$\left(\frac{du}{d\phi}\right)^2 = u^2\left[\frac{E^2 r_0^{\,2}}{\ell^2} - \left(\frac{1-bu}{r_0}\right)\left(-\frac{r_o^{\,2}\varepsilon}{u\ell^2} + r_0\right)\right] \tag{3.12}$$

As can be seen in the later sections, this equation is going to be used in the analysis of the circular motion.

3.2 Radial Geodesics without Angular Momentum

In the case of zero angular momentum (i.e. $\ell = 0$), the motion remains in the plane with $\phi = const.$, and the particle moves only in the radial direction. Therefore, Eq. (3.7) becomes

$$\left(\frac{dr}{d\sigma}\right)^2 = E^2 + \varepsilon f \tag{3.13}$$

In the null geodesics, which refers to the motion of a photon (massless particle), the above equation reduces to

$$\left(\frac{dr}{d\sigma}\right)^2 = E^2 \tag{3.14}$$

Recalling Eq. (3.5), one can change the variable of the above differential equation from the affine parameter σ to the t time. To this end, we use $d\sigma = -\frac{f}{E}dt$ and therefore Eq. (3.14) becomes

$$\frac{dr}{dt} = \pm f = \pm\left(\frac{r-b}{r_o}\right) \tag{3.15}$$

Hence, we first obtain the following integral between the radial position of the photon and the time, and then the solution of $r(t)$ as follows.

$$\begin{aligned}
&\frac{dr}{f} = \pm dt \rightarrow \int \frac{dr}{f} = \pm \int dt \\
&\rightarrow r_o \; ln\left(r-b\right) - ln(c) = \pm\left(t-t_o\right) = \pm\Delta t \\
&\rightarrow ln\left(\frac{r-b}{c}\right) = \pm\frac{\Delta t}{r_o} \\
&\Rightarrow r\left(t\right) = b + c\, exp\left(\pm\frac{\Delta t}{r_o}\right) \\
&r\left(t\right) = r_i + b\left[1 - exp\left(\pm\frac{\Delta t}{r_o}\right)\right]
\end{aligned} \tag{3.16}$$

in which the integral constant c is chosen to be

$$c = r_i - b \geq 0 \tag{3.17}$$

where r_i represents the initial position of the photon, and t corresponds to the time measured by an external observer as his/her initial time is t_0.

On the other hand, in the case of timelike geodesics $\left(i.e.\ \varepsilon = -1\right)$, which belongs to the motion of a massive particle (with unit mass), Eq. (3.13) takes the following form

$$\left(\frac{dr}{d\sigma}\right)^2 = E^2 - f = \frac{E^2 r_o + b - r}{r_o} \tag{3.18}$$

which leads to

$$2\frac{dr}{d\sigma}\frac{d^2r}{d\sigma^2} = -\frac{1}{r_o}\frac{dr}{d\sigma}$$
$$\Rightarrow \frac{d^2r}{d\sigma^2} = -\frac{1}{2r_o} \tag{3.19}$$

If we select the proper time τ, instead of the affine parameter σ, we obtain the radial force per unit mass as

$$\frac{d^2r}{d\tau^2} = a_r = -\frac{1}{2r_o} \tag{3.20}$$

where a_r represents the centrifugal acceleration due to its negative sign. It is well-known that a_r is directed toward centre of the LDBH.

Now let us consider a particle that starts its motion from rest at an initial radial point $r = r_i$. Using $\sigma = \tau$ within Eq. (3.18), we obtain

$$E^2 = \frac{r_i - b}{r_o} \tag{3.21}$$

which changes Eq. (3.18) to

$$\left(\frac{dr}{d\tau}\right)^2 = \frac{r_i - r}{r_o} \tag{3.22}$$

Furthermore, the effective potential in radial motion can be derived from Eq. (3.20). To this end, let us consider the conservative force definition for a test particle ($m = 1$)

$$F = m\frac{d^2r}{d\tau^2} \equiv \frac{d^2r}{d\tau^2} = -\frac{1}{2r_o}$$
$$F = -\nabla V_{eff} \Rightarrow F = -\frac{dV_{eff}}{dr}$$
$$\Rightarrow V_{eff} = -\int F\, dr = \int \frac{1}{2r_o} dr = \frac{r}{2r_0} + c_1 \qquad (3.23)$$
$$V_{eff} = \frac{1}{2r_o}(r - b) = \frac{f}{2}$$

where the integration constant c_1 is properly selected as $c_1 = -\frac{b}{2r_0}$ for the sake of the conformity with Eq. (3.9).

By using the physical quantities given in chapter one, which are $b = 4M$ and $r_0 = \sqrt{2}Q$, the effective potential becomes

$$V_{eff} = \frac{1}{2\sqrt{2}}\left(\frac{r}{Q} - \frac{4M}{Q}\right) \qquad (3.24)$$

Upon introducing $\frac{r}{Q} = \hat{r}$ and $\frac{M}{Q} = \hat{M}$, we can rewrite it as

$$V_{eff}(\hat{r}) = \frac{1}{2\sqrt{2}}\left(\hat{r} - 4\hat{M}\right) \qquad (3.25)$$

which is depicted in Fig. 1. In this figure the horizon $\hat{r}_h$ is the intersection of $V_{eff}(\hat{r})$ with the $\hat{r}$ axis. This figure shows that there is an upper bound for the motion of the particle which tends to diverge while shifting towards spatial infinity. Depending on the bigness of the size of $\hat{M}$ this upper bound diverges further away.

Finally, by using Eqs. (3.5) and (3.13), we can obtain

$$\left(\frac{dr}{dt}\right)^2 = \frac{f^2}{E^2}\left(E^2 - f\right) \qquad (3.26)$$

which is for the timelike geodesics. Now differentiating the square-rooted form of the above expression with respect to t, one finds out that

$$\frac{dr}{dt}=\sqrt{\frac{f^2}{E^2}\left(E^2-f\right)}=\left(X\right)^{\frac{1}{2}}\Rightarrow\left\{X=f^2-\frac{f^3}{E^2}\right\}$$

$$\frac{d^2r}{dt^2}=\frac{d}{dt}\left(X\right)^{\frac{1}{2}}$$

$$\frac{d^2r}{dt^2}=\frac{1}{2}\left(X\right)^{-\frac{1}{2}}\frac{dX}{dt}$$

$$\frac{d^2r}{dt^2}=\frac{1}{2}\left(X\right)^{-\frac{1}{2}}\frac{dX}{dr}\frac{dr}{dt}=\frac{1}{2}\frac{dX}{dr},$$

$$\left\{\frac{dX}{dr}=\left(2f-\frac{3f^2}{E^2}\right)\frac{df}{dr};\quad\frac{df}{dr}=\frac{1}{r_o}\right\},\tag{3.27}$$

$$\frac{d^2r}{dt^2}=\frac{f}{2E^2r_o}\left(2E^2-3f\right)$$

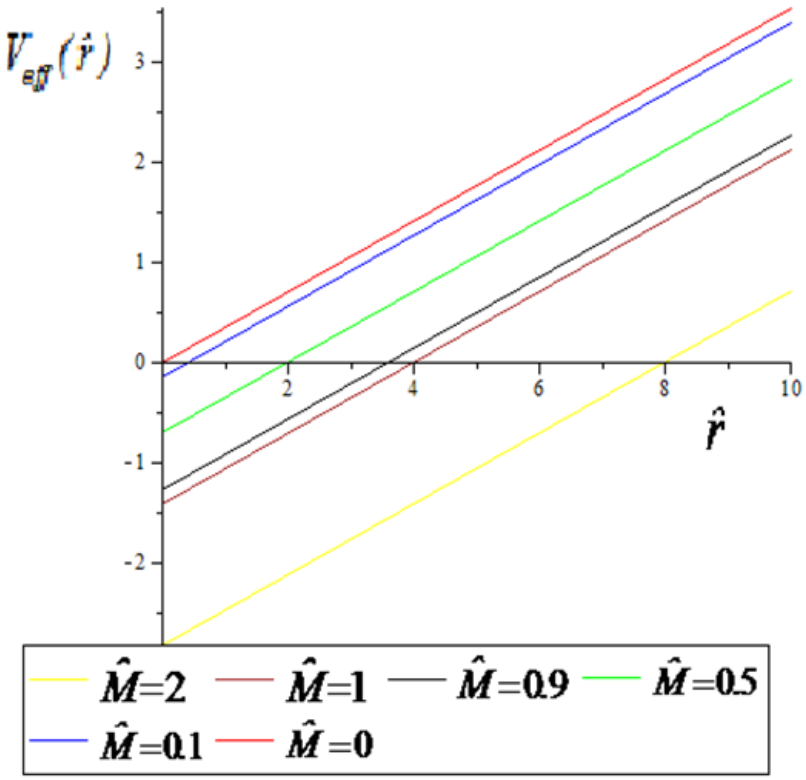

Figure 1: The plot of the effective potential $V_{eff}(\hat{r})$ versus $\hat{r}$. The plot is governed by [Eq. (3.25)]. For a constant $\hat{M}$, the linear behavior of the $V_{eff}(\hat{r})$ is illustrated

In Fig. 2, we plot the variation of the coordinate time (t) and the proper time (τ) along a timelike radial-geodesic described by the test particle, starting at rest at $r = r_i$ and falling towards the centre of the BH (singularity).

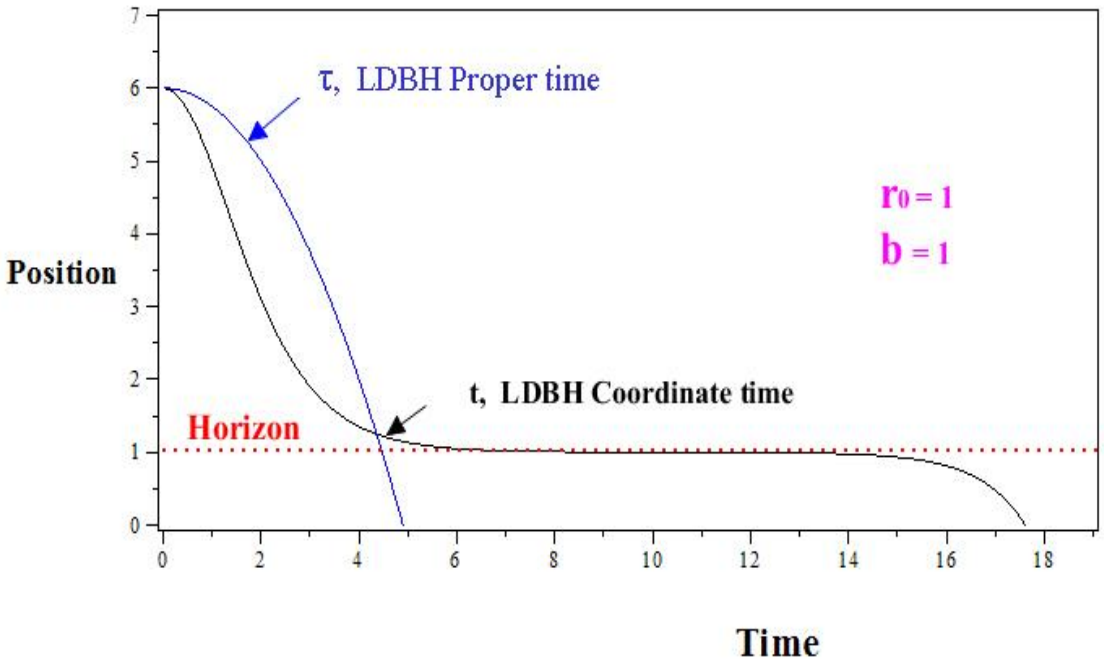

Figure 2: Plot of how the massive particle falls into $r = 0$ singularity of the LDBH spacetime. The plots are governed by Eqs. (3.20) and (3.27).

Also, we would like to emphasize that energy-related constant of motion of the particle can be found from Eq. (3.2). Name6ly, for a massive particle starting from rest, one reads

$$0 = \frac{f_i^2}{E^2}\left(E^2 - f_i\right) \tag{3.28}$$

which yields

$$E^2 = f_i = \frac{r_i - b}{r_o} \tag{3.29}$$

In Fig. 3, we plot E^2 versus r_i for different values of r_0. It is clear from this figure that energy vanishes at the horizon $r_i = b$, which is chosen as 1 in this figure..

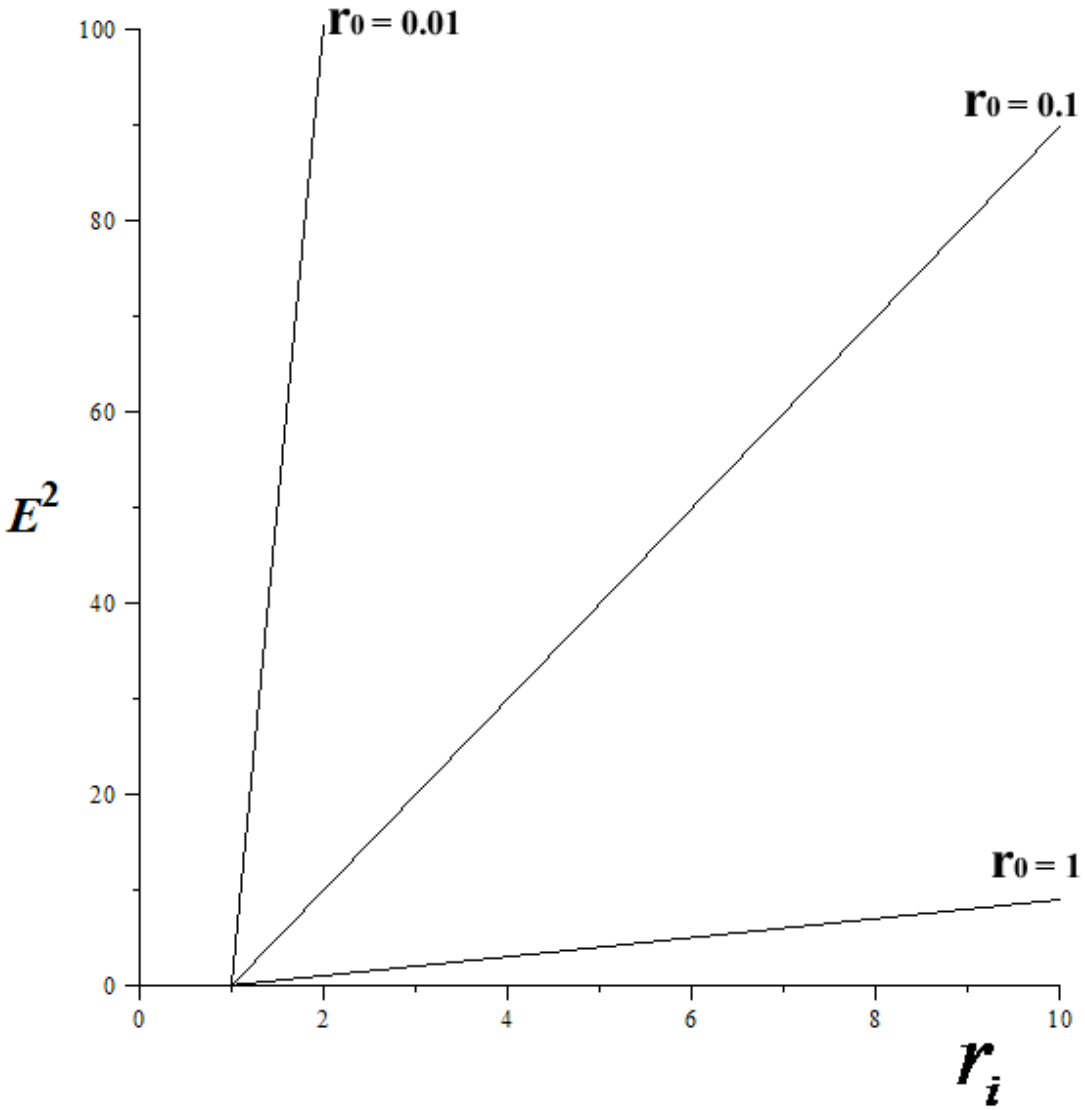

Figure 3: A plot E^2 versus r_i [Eq. (3.29)] of a massive particle, starting from rest at r_i, which moves along timelike geodesics for different values of r_0. Here b=1.

Chapter 4

CIRCULAR GEODESICS OF THE LDBH

4.1 Geodesics with Angular Momentum

In this section, we study the circular motion of both null and timelike geodesics [see Eq. (3.12)] by considering $\left.\frac{du}{d\phi}\right|_{u=uc}=0$ in which $r_c=u_c^{-1}$ is the circular orbit of the particle. Therefore, the associated condition corresponds to

$$\left.\left(\frac{du}{d\phi}\right)^2\right|_{u=u_c}=u_c{}^2\left[\frac{E^2r_o{}^2}{\ell^2}-\left(\frac{1-bu_c}{r_o}\right)\left(r_o-\frac{r_o{}^2\varepsilon}{u_c\ell^2}\right)\right]=0. \tag{4.1}$$

Now, taking derivative of both sides with respect to ϕ one finds

$$2\left(\frac{du}{d\phi}\right)\left(\frac{d^2u}{d\phi^2}\right)=\frac{d}{d\phi}\left\{u^2\left[\frac{E^2r_o{}^2}{\ell^2}-\left(\frac{1-bu}{r_o}\right)\left(r_o-\frac{r_o{}^2\varepsilon}{u\ell^2}\right)\right]\right\} \tag{4.2}$$

which results in

$$\frac{d^2u}{d\phi^2}=\frac{1}{2}\frac{d}{du}\left\{u^2\left[\frac{E^2r_o{}^2}{\ell^2}-\left(\frac{1-bu}{r_o}\right)\left(r_o-\frac{r_o{}^2\varepsilon}{u\ell^2}\right)\right]\right\} \tag{4.3}$$

As usual, the above equation is used for having equilibrium. Namely, the net force exerting on the particle should be terminated. This in turn implies the vanishing of the acceleration, i.e., $\frac{d^2u}{d\phi^2}=0$. Thus we have

$$\frac{d}{du}\left\{u^2\left[\frac{E^2 r_o{}^2}{\ell^2}-\left(\frac{1-bu}{r_o}\right)\left(r_o-\frac{r_o{}^2\varepsilon}{u\ell^2}\right)\right]\right\}\Bigg|_{u=u_c}=0 \tag{4.4}$$

which yields the following expressions for the constants of motion that are required for having the equilibrium.

$$E^2 \equiv E_{eq}^2 = \frac{\varepsilon\left(1-bu_c\right)^2}{u_c{}^2 r_o b} \tag{4.5}$$

and

$$\ell^2 \equiv \ell_{eq}^2 = -\frac{r_o\left(2E_{eq}^2 u_c r_o+\varepsilon-2bu_c\varepsilon\right)}{u_c\left(3bu_c-2\right)} \tag{4.6}$$

Substituting Eq. (4.5) into Eq. (4.6), we further obtain

$$\begin{aligned}
\ell_{eq}^2 &= -\frac{r_o\left(2E_{eq}^2 u_c r_o+\varepsilon-2bu_c\varepsilon\right)}{u_c\left(3bu_c-2\right)} \\
&= -\frac{r_o\left(\dfrac{2u_c r_o\varepsilon\left(1-bu_c\right)^2}{u_c{}^2 br_o}+\varepsilon-2bu_c\varepsilon\right)}{u_c\left(3bu_c-2\right)} \\
&= \frac{-\varepsilon r_o}{u_c\left(3bu_c-2\right)}\left[\frac{2r_o\left(1-bu_c\right)^2}{u_c r_o b}+1-2bu_c\right] \\
&= \frac{-\varepsilon r_o}{u_c\left(3bu_c-2\right)}\left[\frac{2r_o\left(1-bu_c\right)^2+u_c r_o b-2b^2 u_c{}^2 r_o}{u_c r_o b}\right] \\
&= \frac{-\varepsilon r_o}{u_c{}^2 r_o b\left(3bu_c-2\right)}\left[2r_o\left(b^2 u_c{}^2+1-2bu_c\right)+u_c r_o b-2b^2 u_c{}^2 r_o\right] \\
&= \frac{-\varepsilon}{u_c{}^2 b\left(3bu_c-2\right)}\left[2r_o-3u_c r_o b\right] \\
&= \frac{-\varepsilon r_o}{u_c{}^2 b\left(3bu_c-2\right)}\left[2-3u_c b\right]\Rightarrow
\end{aligned}$$

$$
\begin{aligned}
\Rightarrow &= \frac{-\varepsilon r_o}{u_c\left(3bu_c-2\right)}\left[\frac{2r_o\left(1-bu_c\right)^2+u_c r_o b-2b^2 u_c{}^2 r_o}{u_c r_o b}\right] \\
&= \frac{-\varepsilon r_o}{u_c{}^2 r_o b\left(3bu_c-2\right)}\left[2r_o\left(b^2 u_c{}^2+1-2bu_c\right)+u_c r_o b-2b^2 u_c{}^2 r_o\right] \\
&= \frac{-\varepsilon}{u_c{}^2 b\left(3bu_c-2\right)}\left[2r_o-3u_c r_o b\right] \qquad (4.7) \\
&= \frac{-\varepsilon r_o}{u_c{}^2 b\left(3bu_c-2\right)}\left[2-3u_c b\right] \\
&\therefore \\
&\ell_{eq}^2 = \frac{\varepsilon r_o}{u_c{}^2 b}
\end{aligned}
$$

It is easy to see that for the physical particles ($\varepsilon = 0,-1$) both E_{eq}^2 and ℓ_{eq}^2 *cannot take positive values*. It means that the stable (equilibrium) circular motion does not exist in the LDBH background. Additionally, if one computes the ratio of $\frac{E_{eq}^2}{\ell_{eq}^2}$, we have

$$\frac{E_{eq}^2}{\ell_{eq}^2} = \frac{\left(1-bu_c\right)^2}{r_0{}^2} \qquad (4.8)$$

which is independent of ε.

4.2 Null Geodesics of the Circular Motion

To analyze the circular motion of the null geodesics, we first set $\varepsilon = 0$ in Eqs. (4.1) and (4.4). Thus, one arrives at

$$\left.\frac{du}{d\phi}\right|_{u=uc} = -\frac{u_c^3 b}{2} = 0 \quad \Rightarrow \quad u_c = 0 \quad \Rightarrow \quad r_c = \infty \qquad (4.9)$$

and according to the ratio (4.8), one reads

$$\frac{E_{eq}^2}{\ell_{eq}^2} = \frac{1}{r_0{}^2} \qquad (4.10)$$

Furthermore, we want to study on the stability of light orbits. To this end, we use the geodesic equation of the null geodesics given in Eq. (3.7). So, the reduced equation $(\varepsilon = 0)$ becomes

$$\frac{1}{\ell^2}\left(\frac{dr}{d\sigma}\right)^2 + \frac{f}{r_o r} = \frac{E^2}{\ell^2} \tag{4.11}$$

Setting $\sigma = \frac{\tilde{\sigma}}{\ell}$ enables us to rewrite the above expression in the following form

$$\left(\frac{dr}{d\tilde{\sigma}}\right)^2 + \tilde{V}_{eff} = \tilde{E}_{eff} \tag{4.12}$$

where

$$\tilde{V}_{eff} = \frac{f}{r_o r} = \frac{4M}{r r_o^{\,2}}\left(\frac{r}{4M} - 1\right) = \frac{1}{\tilde{r} r_o^{\,2}}\left(\tilde{r} - 1\right) \tag{4.13}$$

$$\tilde{E}_{eff} = \frac{E^2}{\ell^2} \tag{4.14}$$

where $\tilde{r} = \frac{r}{4M}$. The stable circular orbits become possible when we have

$$\left.\frac{d\tilde{V}_{eff}}{dr}\right|_{r=r_c} = 0 \quad \oplus \quad \left.\frac{d^2\tilde{V}_{eff}}{dr^2}\right|_{r=r_c} > 0 \tag{4.15}$$

The peak value of $\tilde{V}_{eff}$ the corresponds to the spatial infinity. Fig. 4 represents the plots for $\tilde{V}_{eff}$ versus $\tilde{r}$ for different values of r_0. These figures manifest that there are no stable circular orbits for photons.

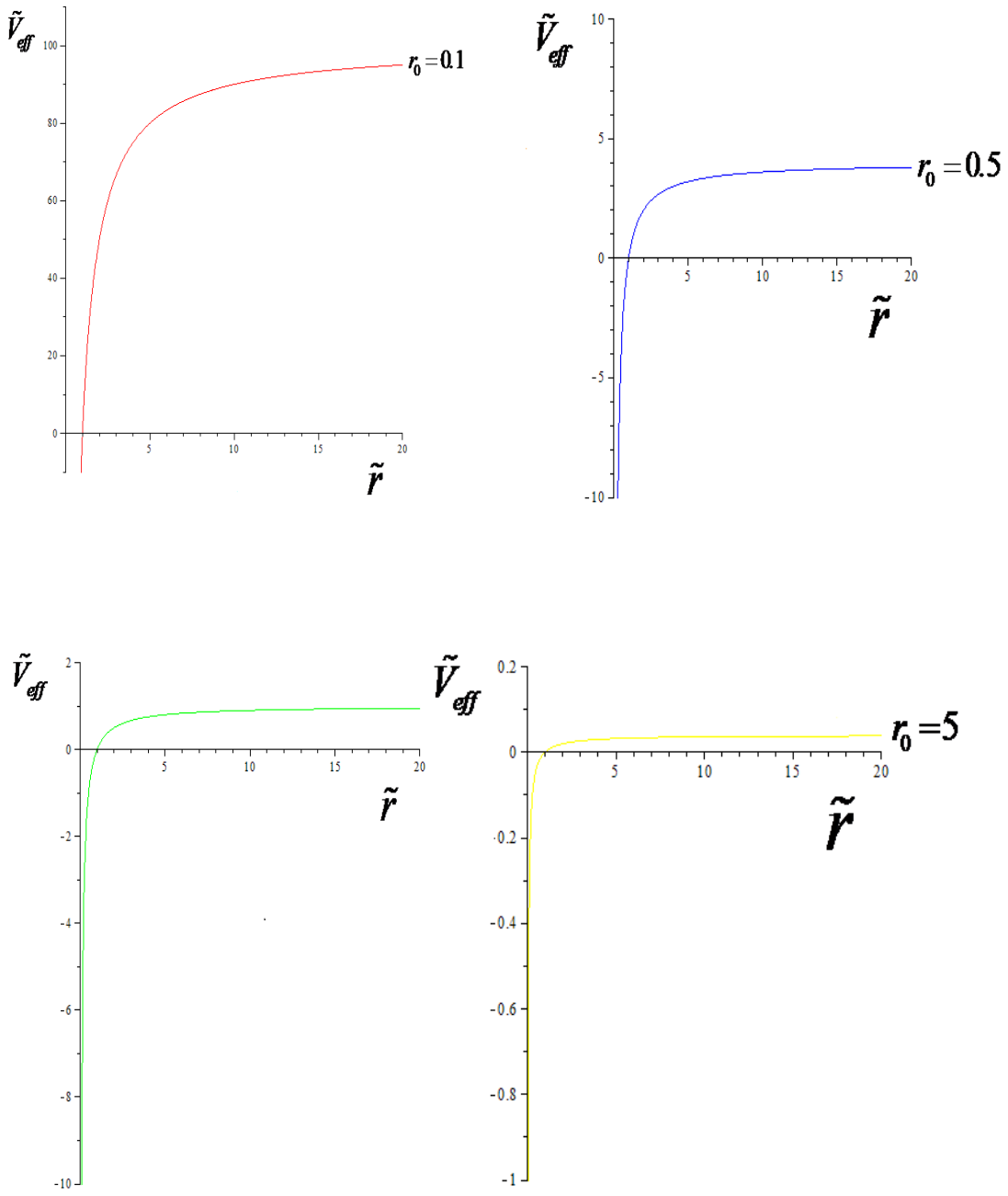

Figure 4: The plot of $\tilde{V}_{eff}$ versus $\tilde{r}$ [see Eq. (4.13)]. For various r_0 values, it is seen that there exists unstable orbits for the massless particles (photons). However, the instability tends to disappear for the greater values r_0 while $\tilde{r} \to \infty$.

For $r_0 = 1$, the orbital motions of the photon are illustrated in Fig. 5.

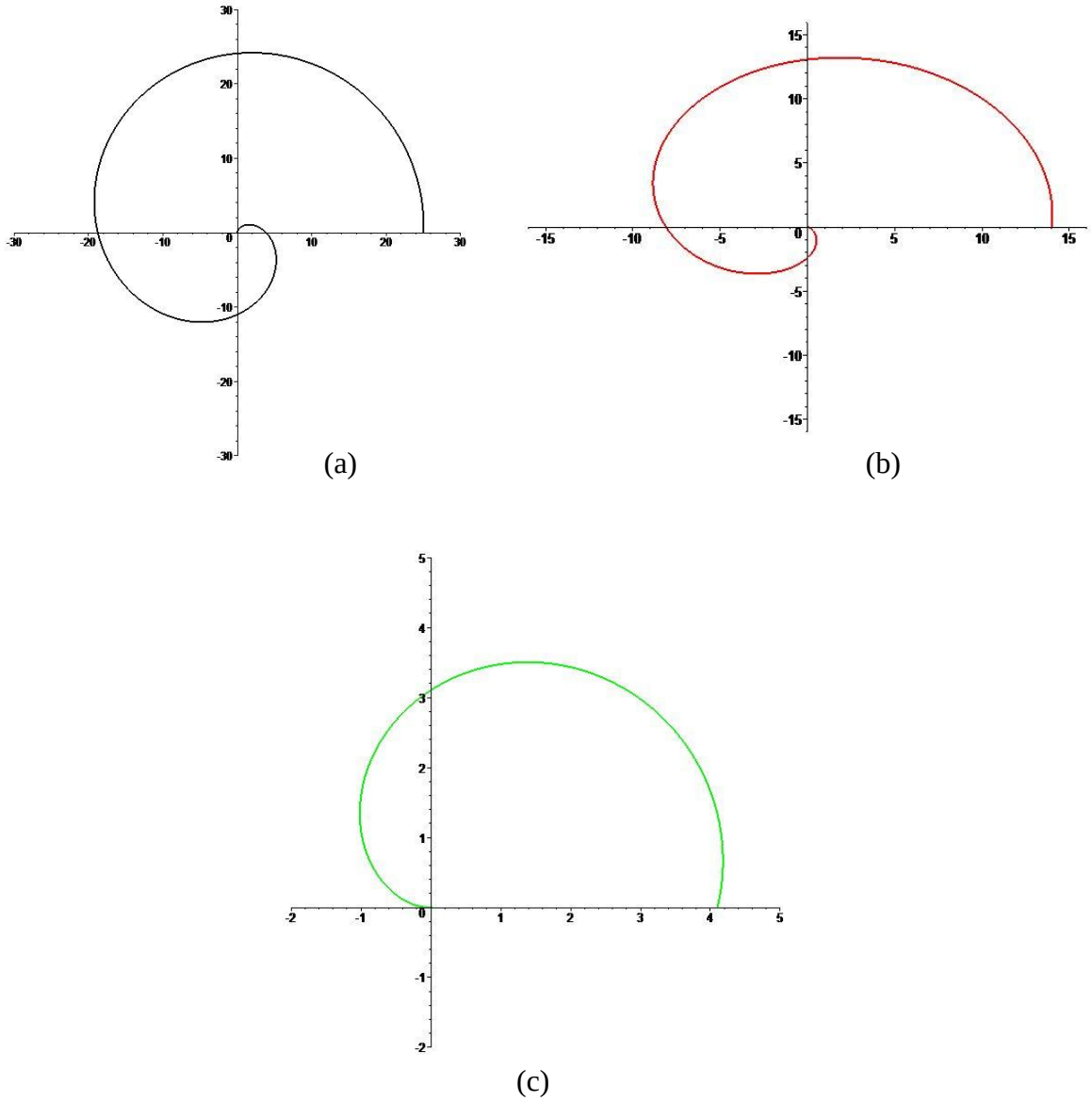

Figure 5: Circular orbits of the photons. The simulations which are made in the famous mathematical program Maple 18 [19] are governed by Eq. (3.11) with $\varepsilon = 0$. During simulations, the initial speed of the photon is assumed to be 1, and the Runge-Kutta method is employed. The far region (a), the middle region (b) and the near horizon region behaviors of the photon are shown. Parameters are chosen to be $M = 1$ $\left(\therefore\ r_h = 4\right)$ and $\ell^2 = 10$.

4.3 Timelike Geodesics of the Circular Motion

To finalize our study about the stability of the equilibrium circular motion for a massive particle, we also take account of the effective potential (3.9) for the dynamical motion of the massive particle. Let us recall that for a stable circular motion the requirements are given in Eq. (4.15). Fig. 6 exhibits the effective potential in terms of $\tilde{r}$ for $r_0 = 0.1, 0.5, 1 \text{ and } 5$, respectively. We see that similar to the unstable circular orbits for the photons, there is no stable circular orbit for the massive particles, whose their plots are presented in detail in the Fig. 7.

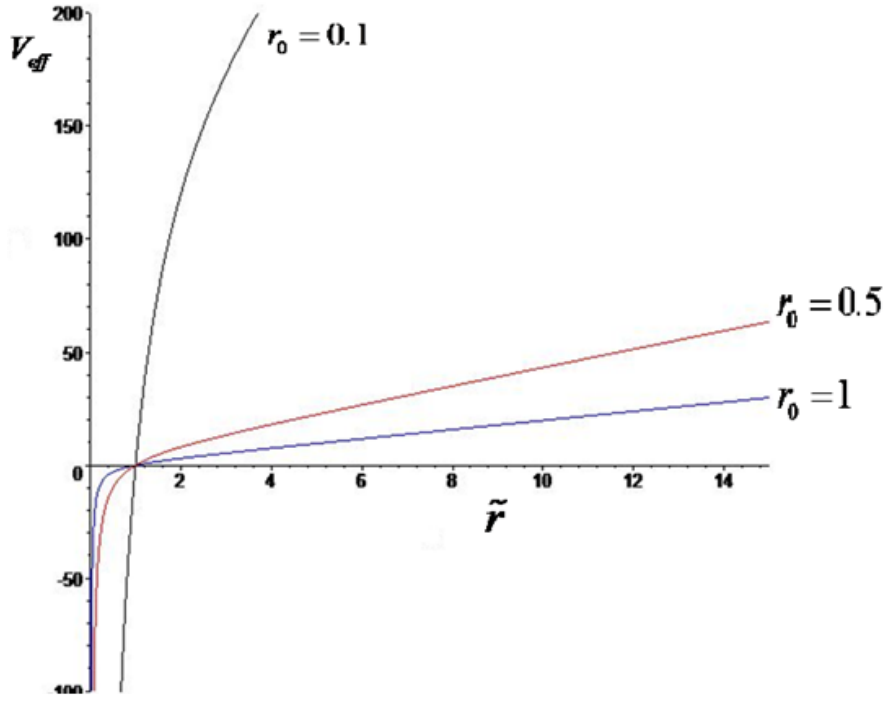

Figure 6: The V_{eff} plot versus $\tilde{r}$ for massive particles with different values of r_0. No stable orbits exist. Here $M = 1$.

In Fig. 7, we give the both plots of the V_{eff} of the massive particles with unit mass and its corresponding circular orbits, in the same framework.

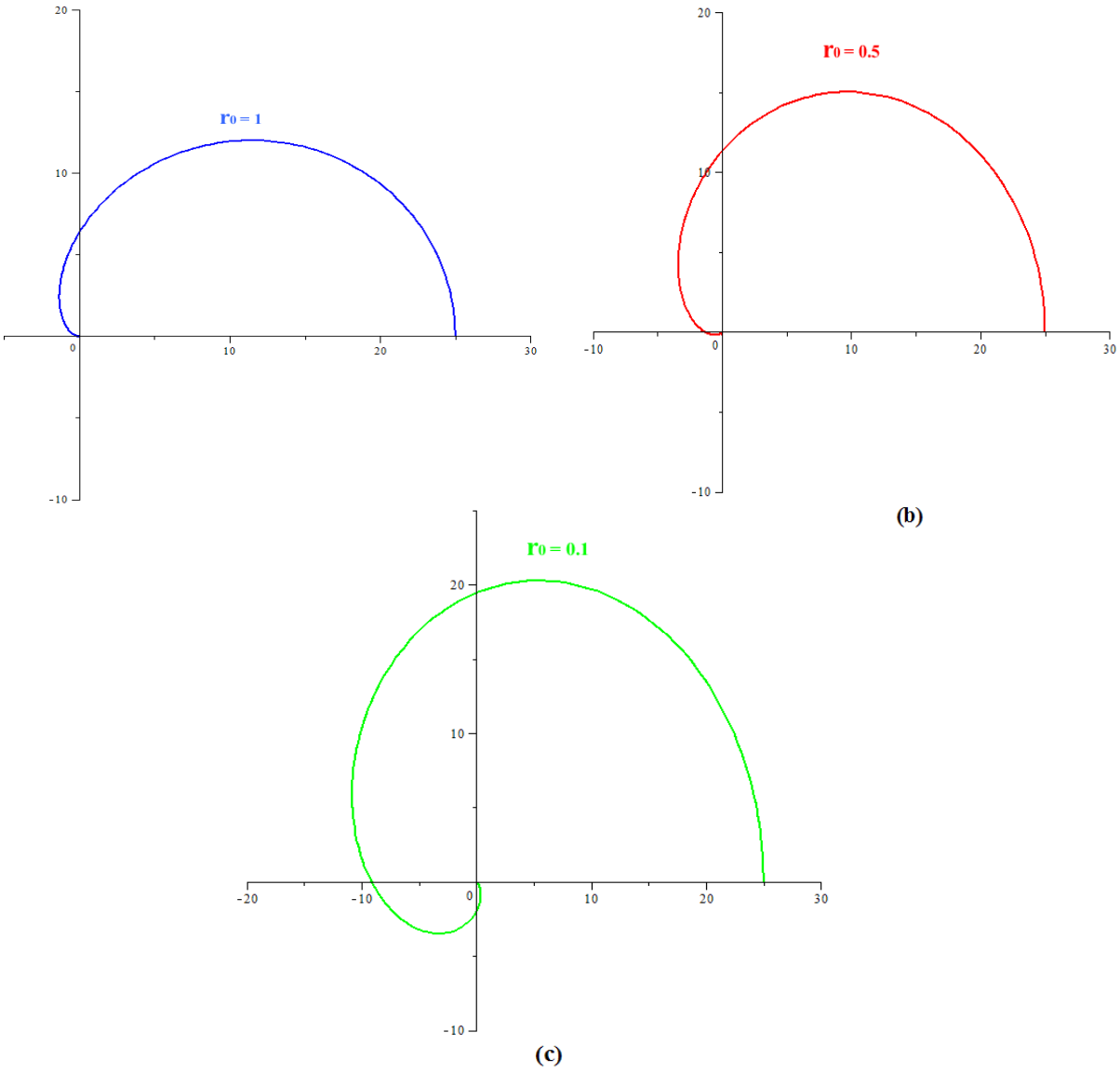

Figure 7: Circular orbits of the massive particles for various r_0 values. The simulations are performed with the Maple 18 [19] and they are governed by Eq. (3.11) with $\varepsilon = -1$. During simulations, the initial speed of the massive particle is assumed to be 0, and the Runge-Kutta method is employed. Parameters are chosen to be $M = 1$ $\left(\therefore\ r_h = 4\right)$ and $\ell^2 = 10$.

Finally, using Eq. (3.20) one can also derive the circular velocity of the massive particles with unit mass by using the fact that $F = \frac{v_{\square}^2}{r}$. Thus one finds

$$v_{\square} = \sqrt{\frac{r}{2r_0}} \tag{4.16}$$

Its associated plots are given in Fig. 8. It can be easily seen that the circular velocity of the massive particles tends to decrease when the charge parameter r_0 gets larger values.

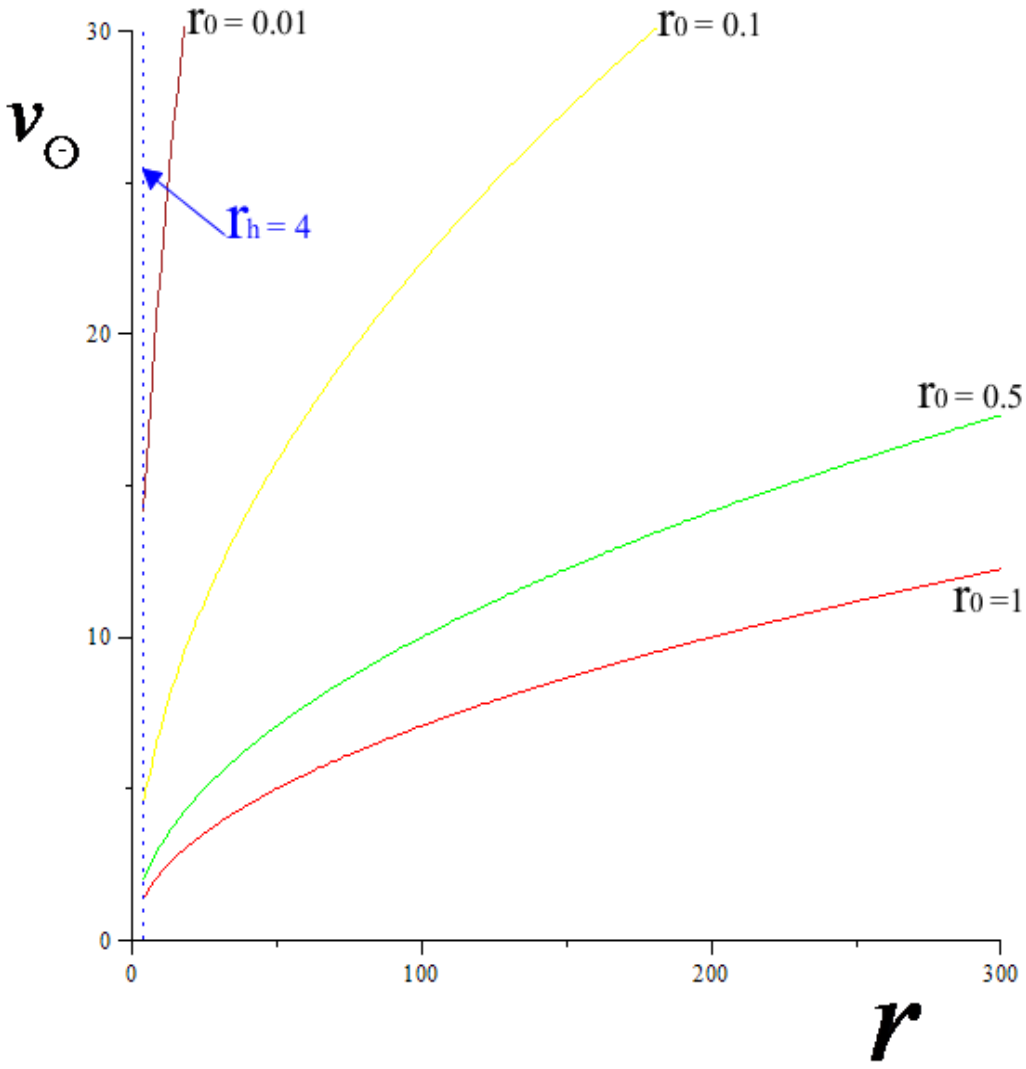

Figure 8: Plots of the circular velocity v_{Θ} versus radial distance r for different values of the r_0. The blue dashed line indicates the event horizon

Chapter 5

ANALYTIC SOLUTION TO THE GEODESIC EQUATIONS OF THE LDBH GEOMETRY

5.1 EL Equations with Mino Proper Time

In this section, we reconsider the Lagrangian (3.1) by using the Mino proper time (γ) [20] which is governed by the following differential expression for the LDBH.

$$d\sigma = rr_0 d\gamma \tag{5.1}$$

Thus, the modified Lagrangian becomes

$$L = -\frac{1}{2}\frac{f}{rr_o}\left(\frac{dt}{d\gamma}\right)^2 + \frac{1}{2rr_o f}\left(\frac{dr}{d\gamma}\right)^2 + \frac{1}{2}\left(\frac{d\theta}{d\gamma}\right)^2 + \frac{1}{2}sin^2\theta\left(\frac{d\phi}{d\gamma}\right)^2 \tag{5.2}$$

and its corresponding metric condition is in the same form with Eq. (3.2). After applying the EL method, we obtain

$$\frac{d}{d\gamma}\left(-\frac{f}{rr_0}\frac{dt}{d\gamma}\right) = 0 \quad \Rightarrow \quad \frac{dt}{d\gamma} = \frac{r^2 r_0}{\Lambda}\alpha \tag{5.3}$$

$$\frac{d}{d\gamma}\left(sin^2\theta\frac{d\phi}{d\gamma}\right) = 0 \quad \Rightarrow \quad \frac{d\phi}{d\gamma} = \frac{\beta}{sin^2\theta} \tag{5.4}$$

in which $\Lambda = rf$, α and β are the integration constants. In addition to them, we have

$$\frac{d^2\theta}{d\gamma^2} = sin\theta cos\theta\left(\frac{d\phi}{d\gamma}\right)^2$$

$$\Rightarrow \quad 2\theta' d\theta' = 2sin\theta cos\theta\left(\frac{d\phi}{d\gamma}\right)^2 d\theta \quad \because \quad \left\{\theta' = \frac{d\theta}{d\gamma}\right\} \tag{5.5}$$

$$\int 2\theta' d\theta' = 2\beta^2 \int \frac{cos\theta}{sin^3\theta} d\theta$$

therefore

$$\left(\frac{d\theta}{d\gamma}\right)^2 = K - \left(\frac{\beta}{sin\theta}\right)^2 \tag{5.6}$$

where K is another integration constant. Finally, with the aid of the metric condition, one can derive the radial equation as follows.

$$-\frac{1}{2}\frac{f}{rr_0}\left(\frac{r^4 r_0^{\,2}}{\Lambda^2}\alpha^2\right) + \frac{1}{2rr_0 f}\dot{r}^2 + \frac{1}{2}\left(K - \frac{\beta^2}{sin^2\theta}\right) + \frac{1}{2}sin^2\theta\frac{\beta^2}{sin^4\theta} = \frac{\varepsilon}{2}$$

$$\Rightarrow -\frac{fr^3 r_0}{r^2 f^2}\alpha^2 + \frac{1}{rr_0 f}\dot{r}^2 + K - \cancel{\frac{\beta^2}{sin^2\theta}} + \cancel{\frac{\beta^2}{sin^2\theta}} = \varepsilon$$

$$\Rightarrow -\frac{r^2 r_0}{\Lambda}\alpha^2 + \frac{1}{\Lambda r_0}\dot{r}^2 = \varepsilon - K \tag{5.7}$$

$$\Rightarrow \dot{r}^2 = (\varepsilon - K)\Lambda r_0 + (\alpha r r_0)^2$$

5.2 Exact Analytical Solution of the Radial Geodesics

Following the method in which the details are given by [21,22], we make a transformation for the r-coordinate as

$$r = \frac{s}{x} + z \tag{5.8}$$

where $s = \pm 1$ and z satisfies the following condition

$$(\varepsilon - K)\Lambda r_0 + (\alpha r r_0)^2\Big|_{r=z} = 0 \tag{5.9}$$

which is equivalent to

$$z^2\left(\alpha^2 r_0{}^2+\varepsilon-K\right)+zb\left(K-\varepsilon\right)=0$$
$$\Rightarrow z=\frac{\Xi}{\Upsilon} \tag{5.10}$$

where

$$\Xi=b\left(\varepsilon-K\right) \tag{5.11}$$

$$\Upsilon=\alpha^2 r_0{}^2+\varepsilon-K \tag{5.12}$$

Then, Eq. (5.7) becomes

$$\left(\frac{dx}{d\gamma}\right)^2=b_3x^3+b_2x^2 \tag{5.13}$$

where

$$b_2=\frac{\alpha^2 r_0{}^2 b}{b-z} \tag{5.14}$$

$$b_3=\frac{z}{s}b_2\equiv szb_2 \tag{5.15}$$

Letting another transformation, which is given by

$$x=\frac{s}{z}\left(\frac{4U}{b_2}-\frac{1}{3}\right) \tag{5.16}$$

we then put Eq. (5.13) into the following form :

$$\left(\frac{dU}{d\gamma}\right)^2=4U^3-\frac{b_2{}^2}{12}+\frac{b_2{}^3}{216} \tag{5.17}$$

The above equation has two solutions. One of them is

$$U_1 = -\frac{b_2}{6} \tag{5.18}$$

which admits $x = -\frac{s}{z}$ and consequently $r = 0$, so that it is a trivial solution. Another solution can be found in terms of the $\wp$-function [15] as

$$U_2 = \frac{1}{6}\wp\left(\frac{\gamma}{\sqrt{6}} + \delta, 3b_2{}^2, -b_2{}^3\right) \tag{5.19}$$

where δ is an integration constant. Thus, the exact solution for the radial geodesics of the LDBH results in

$$r = \frac{s}{x} + z = z\left(\frac{3sb_2}{12U_2 - b_2} + 1\right) \tag{5.20}$$

After a straightforward computational simplifications, we have managed to express it as follows.

$$r = r(\gamma) = \Xi\left[\frac{1}{\Upsilon} - \frac{3}{\Upsilon - 2\wp\left(\frac{\gamma}{\sqrt{6}} + \delta, 3\Upsilon^2, -\Upsilon^3\right)}\right] \tag{5.21}$$

The significant cases about this solution are summarized below.

(i) If $\Xi = 0$, which means that $K = \varepsilon \implies r(\gamma) = 0.$

(ii) If $\Upsilon = 0$, which means that $K = \alpha^2 r_o{}^2 + \varepsilon \implies r(\gamma) \to \infty.$

5.3 Exact Analytical Solution of the Angular Geodesics

One can easily integrate the θ-equation (5.6) to obtain the analytical solution as in the following form.

$$\theta = \theta(\gamma) = \pi \pm \cos^{-1}(\zeta) \tag{5.22}$$

in which

$$\zeta = \sqrt{\beta}\,(\gamma + \hat{\mu}) \tag{5.23}$$

where $\hat{\mu}$ is yet another integration constant. After substituting the above solution into the ϕ-equation (5.4), we find out

$$\phi = \phi(\gamma) = \phi_0 + \sqrt{\beta}\zeta \tag{5.24}$$

where ϕ_0 is also an integration constant.

Chapter 6

CONCLUSION

In this thesis, we have considered geodesic structure of the LDBH, which is a solution to the EMD theory. Using the conventional Lagrangian procedure, the radial and angular geodesics of photons and massive test particles have been obtained. Then, we have studied the radial and circular motions, numerically. We have shown that the effective potentials of both null and timelike geodesics admits unstable motions. The associated circular motion of the photon is exhibited in Fig. (5). Furthermore, depending on the initial position of the massive particle, its spiral like attractive trajectories have been depicted in the Figs. (7). Besides, the circular velocity of the massive particles is also examined. Finally, the exact analytical solution of the general $(\varepsilon = 0,-1,1)$ radial geodesics with the particular time, which is the so-called Mino proper time is given in terms of the $\wp$-function. Also, we have represented the angular solutions as a function of the Mino time.

As a final remark, it would be interesting to extend my work to the geodesics of the rotating LDBHs. Because of this reason, I plan to investigate the effect of the rotation parameter on the related geodesics. This is going to be my future study in the near future.

REFERENCES

[1] Slezakova, G. (2008). Geodesics Geometry of Black Holes. *VDM Verlag Press*, Berlin, Germany.

[2] Hackmann, E., Kagramanova, V., Kunz, J., & Lammerzahl, C. (2009). Analytic Solutions of the Geodesic Equation in Axially Symmetric Space-times. *Europhys. Lett. 88,* 30008.

[3] Hackmann, E., Kagramanova, V., Kunz, J., & Lammerzahl, C. (2010). Analytic solutions of the geodesic equation in Kerr–(anti-)de Sitter space–times. *Phys. Rev. D 81,* 044020.

[4] Hackmann, E., Kagramanova, V., Lammerzahl, C., & Sirimachan, P. (2010). The complete set of solutions of the geodesic equations in the space-time of a Schwarzschild black hole pierced by a cosmic string. *Phys. Rev. D 81,* 064016.

[5] Halilsoy, M., Gurtug, O., & Mazharimousavi, S.H. (2013). Rindler Modified Schwarzschild Geodesics. *Gen. Relativ. Gravit. 45*, 2363.

[6] Clément, G., Galtsov, D., & Leygnac, C. (2003). Linear Dilaton Black Holes. *Phys. Rev. D 67*, 024012.

[7] Chan, K. C. K., Horne, J. H., & Mann, R. B. (1995). Spinning Black Holes in (2+1)-Dimensional String and Dilaton Gravity. *Nucl. Phys. B*, 447.

[8] Pasaoglu, H., & Sakalli, I., (2009). Hawking Radiation of Linear Dilaton Black Holes in Various Theories. *Int. Jour. Theor. Phys. 48*, 3517.

[9] Mazharimousavi, S.H., Sakalli, I., & Halilsoy, M. (2009). Effect of the Born–Infeld Parameter in Higher Dimensional Hawking Radiation. *Phys. Lett. B 672,* 177.

[10] Sakalli, I., Halilsoy, M., & Pasaoglu, H. (2011). Entropy Conservation of Linear Dilaton Black Holes in Quantum Corrected Hawking Radiation. *Int. Jour. Theor. Phys. 50*, 3212.

[11] Sakalli, I., Halilsoy, M., & Pasaoglu, H. (2012). Fading Hawking Radiation. *Astrophys. Space Sci. 340*, 155.

[12] Sakalli, I. (2011). Quantization of Higher Dimensional Linear Dilaton Black Hole Area/entropy From Quasinormal Modes. *Int. J. Mod. Phys. A 26*, 2263; *28*, 1392002 (2013, Erratum).

[13] Sakalli, I., & Mirekhtiary, S.F. (2013). Effect of the Refractive Index on the Hawking Temperature: An Application of the Hamilton-Jacobi Method. *Jour. Exp. Theor. Phys. 117*, 656.

[14] Sakalli, I., Ovgun, A., & Mirekhtiary, S.F. (2014). Gravitational Lensing Effect on the Hawking Radiation of Dyonic Black Holes. *Int. J. Geom. Methods Mod. Phys.* DOI: 10.1142/S0219887814500741

[15] Markushevich, A.I. (1967). Theory of Functions of a Complex Variable. *Prentice-Hall*, Englewood Cliffs, USA.

[16] Brown, J.D., & York, J.W. (1993). Quasilocal Energy and Conserved Charges Derived From the Gravitational Action. *Phys. Rev. D 47,* 1407.

[17] Wald, R.M. (1984). General Relativity. *The University of Chicago Press*, Chicago, USA.

[18] Chandrasekhar, S. (1983). The Mathematical Theory of Black Holes. *Oxford University Press*, Oxford, UK.

[19] Maplesoft. (2014). Maple 18. *Waterloo Maple Inc.*, Waterloo, Ontario, Canada.

[20] Mino, Y. (2003). Perturbative Approach to an Orbital Evolution Around a Supermassive Black Hole. *Phys. Rev. D 67,* 084027.

[21] Kagramanova, V., Kunz, J., V.,Hackmann, E., & Lammerzahl, C. (2010). Analytic treatment of complete and incomplete geodesics in Taub-NUT space-times. *Phys. Rev. D 81*, 124044.

[22] Grunau, S., & Kagramanova, V. (2011). Geodesics of electrically and magnetically charged test particles in the Reissner-Nordström space-time: Analytical solutions *Phys. Rev. D 83,* 044009.